P5.3 VERTICAL STRUCTURE AND CHARACTERISTICS OF TWO LEADING STRATIFORM MESOSCALE CONVECTIVE SYSTEMS

Crystalyne R. Pettet* and Richard H. Johnson
Colorado State University, Fort Collins, Colorado

1 INTRODUCTION

Parker and Johnson (2000) documented three classes of linear mesoscale convective system (MCS) organization: a convective line with trailing stratiform (TS) (defined by Houze et al. 1990), leading stratiform (LS), and parallel stratiform (PS) precipitation. While numerous studies have documented the structure of TS MCSs, the two other modes have received little attention. The reflectivity structure of LS storms looks like a mirror image of TS systems, although they are shorter-lived. However, it is not known if the circulation features are similarly related. Parker and Johnson (2000) show that the convective cells in LS systems are fed in one of two ways: a front-to-rear (FTR) flow that has passed through the stratiform rain ahead of the convection, or a rear-to-front (RTF) flow from behind the system. This study investigates two of the latter LS cases: a 30 April 2000 storm in Oklahoma (Fig. 1), and a 7 May 1997 system in South Dakota and Iowa (Fig. 2). To compare these LS observations to TS storms, it is necessary to review typical TS structure.

Trailing stratiform MCSs have a descending rear inflow jet (Smull and Houze 1987) that passes through the stratiform region and down to the surface, eventually reversing when it encounters the convective cells. This rain-cooled air does not enter the updraft in the leading convective line. Trailing stratiform MCSs are fed from the front, with air that has not been tainted by previous rain. There is a strong rising FTR flow behind the convective cells which carries hydrometeors to the rear of the storm, forming the trailing stratiform rain (Smull and Houze 1985; Rutledge and Houze 1987). As the ice crystals grow they begin to fall and melt, forming a region of enhanced reflectivity just below the freezing level known as the bright band (Houze et al. 1989). Trailing stratiform systems often develop a surface cold pool beneath their convective cores that

**Corresponding author address:* Crystalyne R. Pettet, Department of Atmospheric Science, Colorado State University, Fort Collins, CO 80523-1371; cliska@thunder.atmos.colostate.edu

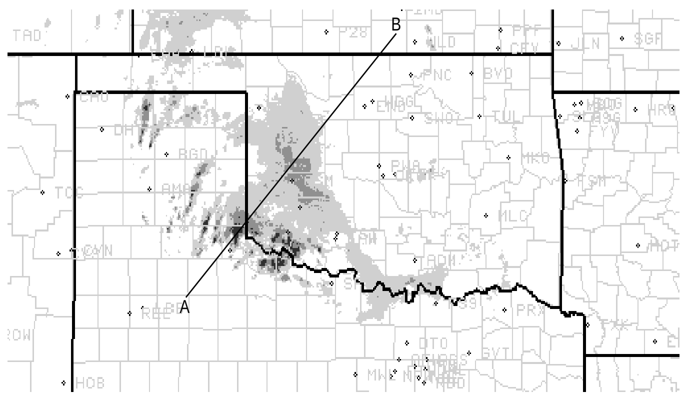

Figure 1: Base-scan radar reflectivity of LS MCS at 1500 UTC on 30 April 2000. Light shading = 20–39dBZ, medium shading 40–49 dBZ, dark shading ≥ 50dBZ. Line A-B is used for Fig. 3 and Fig. 6.

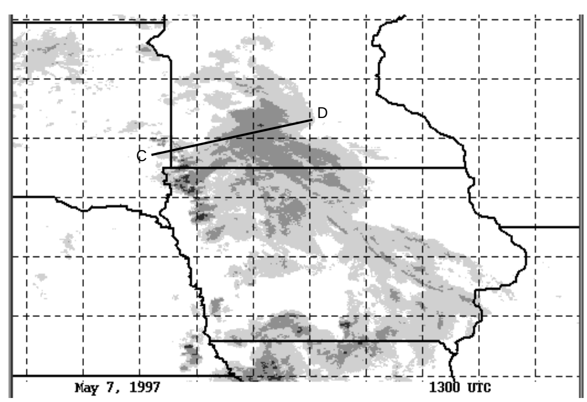

Figure 2: Base-scan radar reflectivity of LS MCS at 1300 UTC on 7 May 1997. Same shading as Fig. 1. Line C-D is used for Fig. 7.

advances ahead of the storm, helping to initiate new cells along the front inflow.

2 DATA

The datasets available for these two cases differed. Wind profiler and Oklahoma mesonet data were used in analyzing the 30 April case, while Doppler radar data were used for the 7 May case. Mesonet and profiler data were gridded using a Barnes objective analysis technique (Barnes 1973; Koch et al. 1983). Doppler radar data were gridded to a 1 km $\times$ 1 km $\times$ 0.5 km grid spacing using a Cressman filter. Time-spatial analyses were also performed on the mesonet data assuming a steady-state of 30 minutes. Vertical cross sections of wind profiler data were taken perpendicular to the line, with storm motion subtracted out to determine storm-relative flow. Vertical cross sections of Doppler radar data were taken along the line of storm motion, again with storm motion subtracted out to determine storm-relative flow. RUC reanalyses and atmospheric soundings were also used for both cases.

3 OBSERVATION AND ANALYSIS

3.1 30 April 2000

Since Doppler radar data were unavailable for the 30 April LS MCS, wind profiler network data were used to construct the vertical profile of the environmental flow. Although these data are coarse relative to Doppler radar data, they supplied the general vertical flow structure for this case. Oklahoma mesonet data were also available, which provided high resolution surface pressure, temperature, and wind speed and direction information. To determine storm-relative flow, a storm motion vector of 9 m s^{-1} toward 32° was used. Vertical cross sections of gridded wind profiler data (Fig. 3), as well as the RUC reanalyses (not shown), show evidence of three primary circulations: RTF flow aloft carrying hydrometeors ahead of the convective line, FTR flow at midlevels (a "leading inflow jet"), and RTF flow at low levels. The RTF flow at low levels is opposite to the surface flow (Fig. 4), a fourth circulation feature, and hence may be considered an elevated rear inflow. This sharp reversal of the low-level flow is associated with a sharp frontal inversion (Oklahoma is north of a quasi-stationary front). With the stratiform precipitation advancing ahead of the convective line, this rear inflow "feeds" the LS convective line high-θ_e air unmodified by rainfall evaporation.

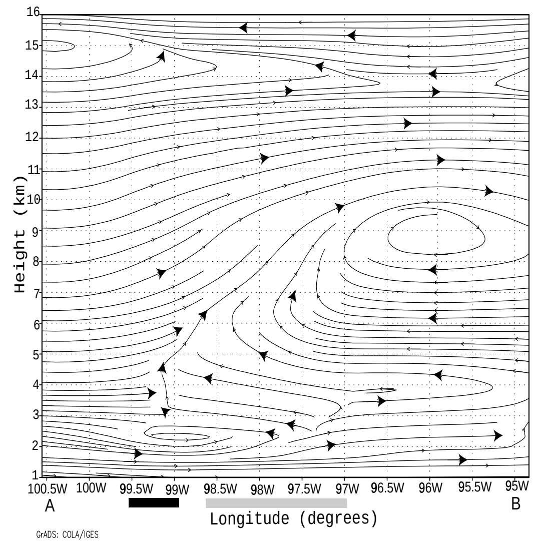

Figure 3: Vertical cross section of profiler-derived storm-relative streamlines along A-B in Fig. 1 for 1500 UTC, 30 April 2000. Black bar indicates convective region, gray bar indicates stratiform region.

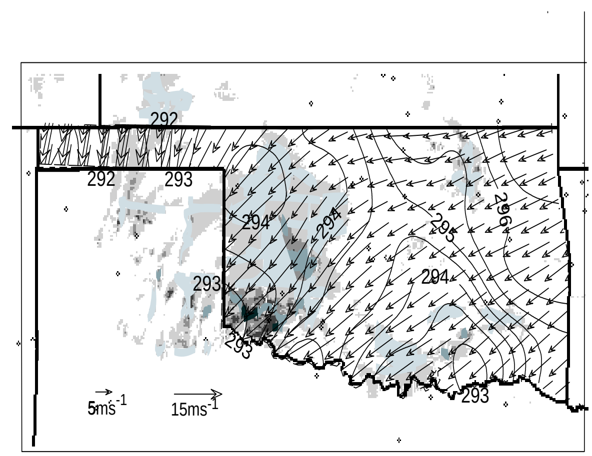

Figure 4: Potential temperature (contour interval 0.5 K) and storm-relative wind vectors at 1600 UTC 30 April 2000 over the Oklahoma mesonet. Radar reflectivity shading as Fig. 1.

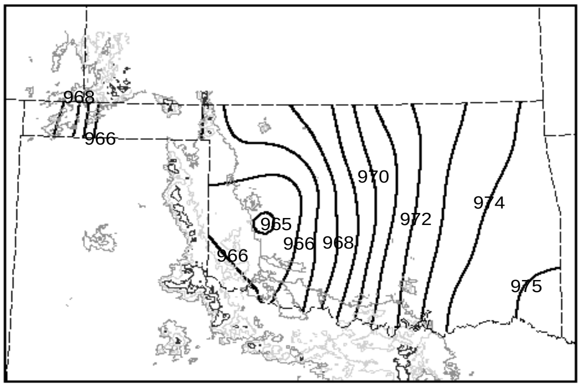

Figure 5: Adjusted station pressure (1 hPa contours) and radar reflectivity contours at 1015 UTC on 30 April 2000. Medium contour = 20–39 dBZ, light contour 40–49 dBZ, dark contour ≥ 50 dBZ.

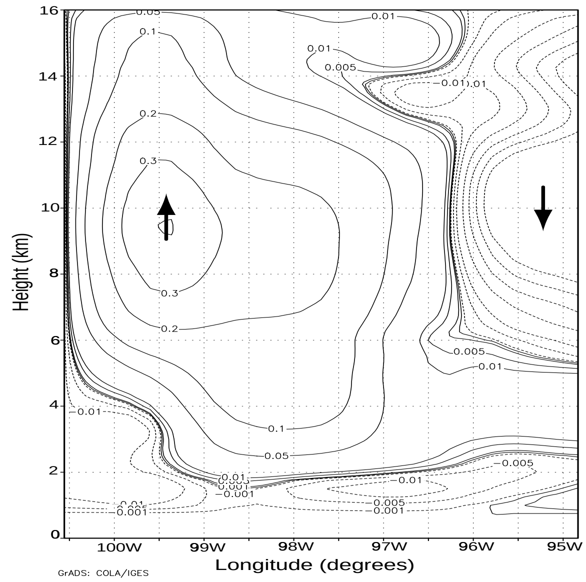

Figure 6: Average vertical velocity (m s^{-1}) derived from gridded wind profiler analysis along A-B in Fig. 1 for 1200–1500 UTC 30 April 2000. Dashed contours represent descending motion, solid contours represent ascending motion.

A leading mesolow can be seen in Fig. 5 which moves to the southeast, along the stratiform area. Further analysis of this mesolow indicates it has gravity wave-like features. A descending leading inflow jet appears in the data (Fig. 6), similar to the rear inflow jet commonly observed in TS systems. This feature could be responsible for heat bursts that occur ahead of and beneath the stratiform area in a manner similar to that described by Johnson (2001).

In a broad sense, most features in the 30 April LS MCS appear as a mirror image of typical TS structure. However, the convective line in this LS system is far more discontinuous. Another distinctive difference found in the mesonet data is the surface flow in the LS. A TS rear inflow jet reverses when it reaches the convective core, with the jet flow being RTF but the surface flow below being FTR in a storm-relative sense. In this LS, however, it is difficult to determine from the coarse profiler data if the FTR leading inflow jet descends and reverses as it reaches the convective region. If the jet does reverse to produce the low-level RTF flow in Fig. 3, the reversal occurs atop a FTR surface flow. The unique aspect of the flow structure of the 30 April case is that the convective line is fed by an elevated rear inflow, decoupled from a reversed surface flow. This low-level flow structure is distinct from TS systems.

3.2 7 May 1997

Doppler radar data were available for the 7 May LS. An analysis of this dataset provides the vertical structure of the storm at a much higher resolution than the 30 April case. A vertical cross section taken along the line shown in Fig. 2 averaged over 10 minutes (3 scans) can be seen in Fig. 7. A storm motion vector of 15 m s^{-1} toward 82° was used to determine storm-relative flow. Doppler radar analyses of storm-relative radial velocity for the 7 May case again indicate the presence of an elevated rear inflow at 3 km AGL (Fig. 7). Nearby soundings at OAX (Fig. 8) and ABR (not shown) show an elevated θ_e maximum at 850 and 800 hPa, respectively. Wind speeds and directions from these soundings show potential rear inflow between 667 and 624 hPa (OAX) and 700 and 664 hPa (ABR). These soundings are consistent with the radar data, showing an elevated region of high θ_e air flowing into the storm. These datasets support the findings of the coarser profiler data in the 30 April case.

Again, there is evidence of descending leading inflow, but it extends to near the surface. The storm-relative radial velocity cross sections also depict rising RTF flow at upper levels which advects hydrometeors downstream to form the stratiform precipitation ahead of the convective line. Numerous vertical cross sections of radar reflectivity show a significant bright band progressing ahead of the convective line with a transition zone of low reflectivity dividing the two areas (not shown). They also show evidence of a small trailing anvil (Fig. 9). This feature also appears as a mirror image of typical TS structure. RUC reanalyses, although they have lower resolu-

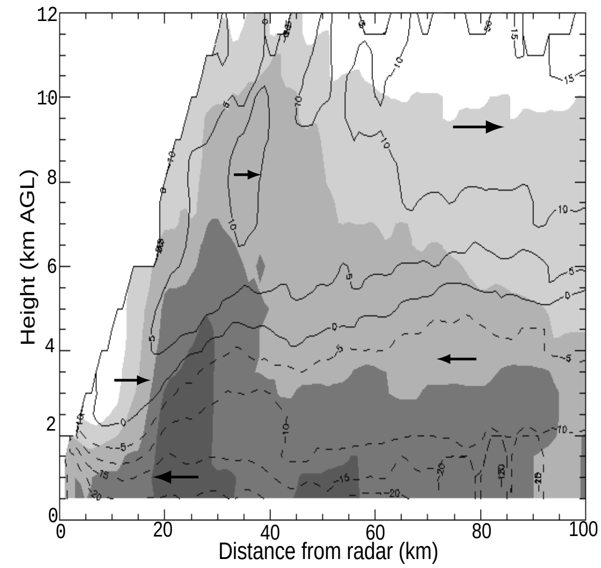

Figure 7: Average vertical cross section of radar reflectivity and storm-relative flow (m s^{-1}) along line C-D in Fig. 2 from 1221 to 1231 UTC on 7 May 1997. Reflectivities are shaded in 10 dBZ increments, lightest is 10 dBZ, darkest is 40 dBZ. Solid contours are away from the radar, dashed contours are toward the radar.

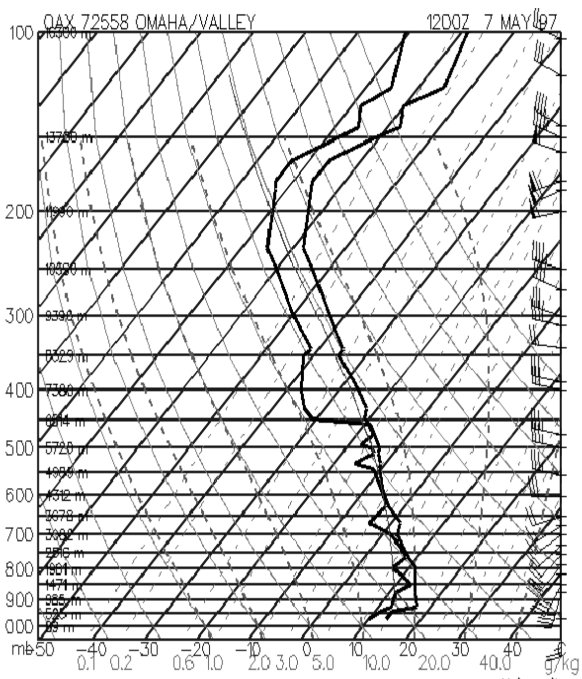

Figure 8: Sounding from Omaha, Nebraska (OAX), at 1200 UTC on 7 May 1997.

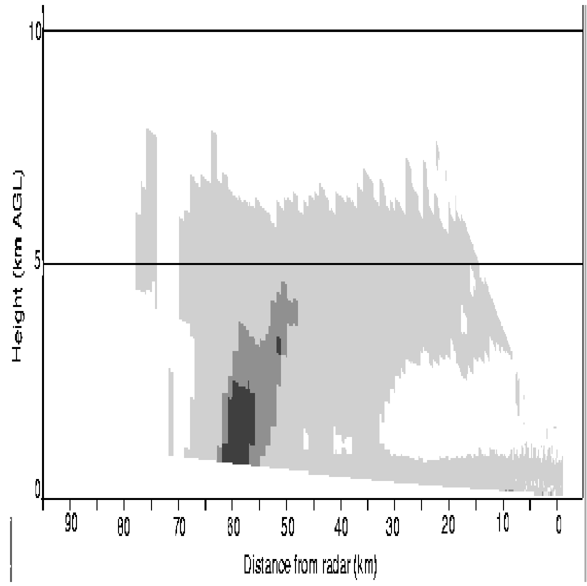

Figure 9: Vertical cross section of radar reflectivity at 0733 UTC on 7 May 1997. Shading as in Fig. 1.

tion than the mesonet data, show a stronger cold pool for the 7 May case than the 30 April case (not shown).

4 SUMMARY

Leading stratiform (LS) MCSs have several features which appear to be mirror images of features in TS MCSs. The LS systems studied here both have a descending leading inflow jet. Both LS systems have ascending RTF flow above the leading inflow jet which carries hydrometeors downstream of the convective cells to form the stratiform precipitation at the front of the system. The 7 May LS shows evidence of a small trailing anvil. It also has an area of enhanced reflectivity located beneath the freezing level in the stratiform region which may be considered to be a bright band.

While practically being a mirror image of TS MCSs in terms of reflectivity, the LS systems studied have some features that are different than typical TS structure. First, the convective lines are far more discontinuous. The individual convective cells are easy to distinguish in both of these cases. Second, both cases are fed from elevated pockets of high-θ_e air that are found behind the storm system. Third, in the 30 April 2000 case, this elevated rear inflow is decoupled from a reversed surface flow, with FTR flow at the surface throughout the storm.

5 ACKNOWLEDGEMENTS

This research has been supported by the National Science Foundation under Grant ATM-0071371 and an American Meteorological Society Graduate Fellowship.

6 REFERENCES

Barnes, S.L., 1973: Mesoscale objective analysis using weighted time-series observations. NOAA Tech. Memo. ERL NSSL-62, National Severe Storms Laboratory, Norman, OK 73069, 60pp. [NTIS COM-73-10781].

Houze, R.A., Jr., S.A. Rutledge, M.I. Biggerstaff, and B.F. Smull, 1989: Interpretation of Doppler weather radar displays of midlatitude mesoscale convective systems. *Bull. Amer. Meteor. Soc.*, **70**, 608-619.

Johnson, R.H., 2001: Surface mesohighs and mesolows. *Bull. Amer. Meteor. Soc.*, **82**, 13-31.

Koch, S.E., M. DesJardins, and P.J. Kocin, 1983: An interactive Barnes objective map analysis scheme for use with satellite and conventional data. *J. Appl. Meteor.*, **22**, 1487-1502.

Parker, M.D., and R.H. Johnson, 2000: Organizational modes of midlatitude mesoscale convective systems. *Mon. Wea. Rev.*, **128**, 3413-3436.

Rutledge, S.A. and R.A. Houze, Jr., 1987: A diagnostic modeling study of the trailing stratiform region of a midlatitude squall line. *J. Atmos. Sci.*, **44**, 2640-2656.

Smull, B.F., and R.A. Houze, Jr., 1985: A midlatitude squall line with a trailing stratiform rain: Radar and satellite observations. *Mon. Wea. Rev.*, **113**, 117-133.

Smull, B.F., and R.A. Houze, Jr., 1987: Rear inflow in squall lines with trailing stratiform precipitation. *Mon. Wea. Rev.*, **115**, 2869-2889.